0026-895X/07/7204-856–867$20.00
MOLECULAR PHARMACOLOGY
Copyright © 2007 The American Society for Pharmacology and Experimental Therapeutics
Mol Pharmacol 72:856–867, 2007

Vol. 72, No. 4
31427/3252852
Printed in U.S.A.

Activation of the Adenosine A_1 Receptor Inhibits HIV-1 Tat-Induced Apoptosis by Reducing Nuclear Factor-κB Activation and Inducible Nitric-Oxide Synthase

Sandeep C. Pingle, Sarvesh Jajoo, Debashree Mukherjea, Lynn F. Sniderhan, Krishna A. Jhaveri, Adriana Marcuzzi, Leonard P. Rybak, Sanjay B. Maggirwar, and Vickram Ramkumar

Departments of Pharmacology (S.J., D.M., K.A.J., V.R.), Medicine (A.M.), and Surgery (D.M., L.P.R.), Southern Illinois University School of Medicine, Springfield, Illinois; Department of Pharmacology, Georgetown University Medical Center, Washington, DC (S.C.P.); and Department of Microbiology and Immunology, University of Rochester Medical Center, Rochester, New York (L.F.S., S.B.M.)

Received October 4, 2006; accepted June 26, 2007

ABSTRACT

Human immunodeficiency virus dementia (HIV-D) is a nonfocal central nervous system manifestation characterized by cognitive, behavioral, and motor abnormalities. The pathophysiology of neuronal damage in HIV-D includes a direct toxic effect of viral proteins on neuronal cells and an indirect effect caused by the release of inflammatory mediators and neurotoxins by activated macrophages/microglia and astrocytes, culminating into neuronal apoptosis. Previous studies have documented that the nucleoside adenosine mediates neuroprotection by activating adenosine A_1 receptor subtype (A_1AR) linked to suppression of neuronal excitability. In this study, we show that A_1AR activation protects against HIV-1 Tat-induced toxicity in primary cultures of rat cerebellar granule neurons and in rat pheochromocytoma (PC12) cell. In PC12 cells, HIV-1 Tat increased $[Ca^{2+}]_i$ levels, release of nitric oxide (NO), and expression of inducible nitric-oxide synthase (iNOS) and A_1AR. Activation of A_1AR suppressed Tat-mediated increases in $[Ca^{2+}]_i$ and NO. Furthermore, A_1AR agonists inhibited iNOS expression in a nuclear factor-κB (NF-κB)-dependent manner. It is noteworthy that activation of the A_1AR or inhibition of NOS protected against Tat-induced apoptosis in PC12 cells and cerebellar granule cells. Moreover, activation of the A_1AR-inhibited Tat-induced increases in the levels of proapoptotic proteins Bax and caspase-3. Taken together, our results demonstrate that the A_1AR protects against HIV-1 toxicity by inhibiting NF-κB, thereby reducing the expression of iNOS and NO radicals and neuronal apoptosis.

HIV dementia (HIV-D) is a syndrome of cognitive and motor dysfunction (Kaul et al., 2001) that occurs late in the course of HIV infection and progresses slowly over months. Its major clinical features include a decline in cognitive and behavioral functions and motor abnormalities. After the introduction of highly active antiretroviral therapy, there was a significant decrease in the incidence of HIV-D. However, because there has been an increase in the number of individuals living with HIV/AIDS due to effective therapy, the prevalence of HIV-D has actually increased.

Even though HIV primarily targets the immune system and produces widespread immunodeficiency, it also affects

This work was supported from the Southern Illinois University School of Medicine Excellence in Academic Medicine Award (to V.R.) and National Institutes of Health grants DC02396 (to L.P.R.), NS054578 (to S.B.M.), and T32-AI49105 (to L.F.S.).

Article, publication date, and citation information can be found at http://molpharm.aspetjournals.org.

doi:10.1124/mol.106.031427.

ABBREVIATIONS: HIV-D, human immunodeficiency virus-dementia; A_1AR, adenosine A_1 receptor; iNOS, inducible nitric-oxide synthase; NF-κB, nuclear factor κB; PC12 cells, pheochromocytoma 12 cells; CGN, cerebellar granule neuron; R-PIA, *R*-phenylisopropyladenosine; DPCPX, 8-cyclopentyl-1,3-di[2′,3′-3*H*] propylxanthine; AR, adenosine receptor; PCR, polymerase chain reaction; PBS, phosphate-buffered saline; RT-PCR, reverse transcription-polymerase chain reaction; bp, base pair; EMSA, electrophoretic mobility shift assay; GAPDH, glyceraldehyde phosphate dehydrogenase; AP-1, activator protein-1; FITC, fluorescein isothiocyanate; TUNEL, terminal deoxynucleotidyl transferase dUTP nick-end labeling; AM, acetoxymethyl ester; L-NAME, N^G-nitro-L-arginine methyl ester; SNAP, *S*-nitroso-*N*-acetylpenicillamine; C-PTIO, 2-(4-carboxyphenyl)-4,4,5,5-tetramethylimidazoline-1-oxyl-3-oxide; OCT-1, octamer transcription factor-1; DAF-2 DA, 4,5-diaminofluorescein diacetate; CHAPS, 3-[(3-cholamidopropyl) dimethylammonio]-1 propanesulfonate; ZM241385, 4-(2-[7-amino-2-(2-furyl)[1,2,4]-triazolo[2,3-*a*] [1,3,5] triazin-5-ylamino]ethyl) phenol; MRS1220, *N*-(9-chloro-2-(2-furanyl)[1,2,4]-triazolol[1,5-*c*]quinazolin-5-benzeneacetamide; BAPTA, 1,2-bis(2-aminophenoxy)ethane-*N,N,N′,N′*-tetraacetic acid; CGS21680, 4-[2-[[6-amino-9-(*N*-ethyl-β-D-ribofuranuronamidosyl)-9*H*-purin-2-yl]amino]ethyl] benzenepropanoic acid.

the central nervous system, resulting in HIV encephalopathy, the pathologic hallmark of HIV-D. There are different theories describing mechanisms of neuronal damage seen in HIV-D, including a direct toxic effect on neurons and an indirect effect mediated by immune cells (Kaul et al., 2001).

Once it enters the central nervous system, HIV productively infects brain macrophages, microglia, and multinucleate giant cells (Kaul et al., 2001), the resident immune cells of the brain, leading to the production of viral proteins such as the envelope glycoprotein gp120, Tat, and the viral proteins Nef and Vpr. These proteins, in previous studies, produce direct neuronal damage by different mechanisms (Kruman et al., 1998; Nath et al., 2000). Infection of immune cells stimulates an inflammatory response, leading to neuronal damage by an indirect or the so-called "bystander" effect (Kaul et al., 2001). Neuronal damage seen in HIV-D probably involves a mixture of the direct and indirect mechanisms (González-Scarano and Martin-Garcia, 2005).

The nucleoside adenosine exerts its major physiological effects by interacting with different subtypes of adenosine receptors (ARs), of which A_1AR is the predominant subtype in the central nervous system (Dunwiddie and Masino, 2001). Previous reports strongly support a cytoprotective role of A_1AR in the central nervous system (Dunwiddie and Masino, 2001; Ramkumar et al., 2001). To date, we are not aware of any study demonstrating a beneficial action of activation of the A_1AR or other ARs against HIV-1 proteins in the central nervous system or in neuronal cultures. However, recent data show that adenosine, acting via A_{2A}AR, inhibits Tat-induced tumor necrosis factor-α production in primary monocytes (Fotheringham et al., 2004).

In this study, we determined whether adenosine analogs could confer protection against HIV-induced toxicity in rat pheochromocytoma (PC) 12 cells and in primary cultures of cerebellar granule neurons (CGNs), used previously to study HIV-1 Tat signaling in vitro (Wong et al., 2005; Sui et al., 2006). HIV-1 Tat was used because this protein can cross the blood-brain barrier (Schwarze et al., 1999), is elevated in patients with HIV-D (Nath et al., 2000), and injection in experimental animals can produce pathological findings similar to those observed in HIV-D (Jones et al., 1998). Our data indicate that activation of the A_1AR protects PC12 cells and CGN cultures from HIV-1 Tat-mediated apoptosis, presumably by inhibiting inducible nitric-oxide synthase (iNOS) expression and NO release via inhibition of nuclear factor (NF)-κB activation.

Materials and Methods

Cell Cultures. Rat pheochromocytoma cells (PC12) were obtained from the American Type Culture Collection (Manassas, VA). Cells were cultured in flasks coated with 0.1 mg/ml poly(D-lysine) (Invitrogen, Carlsbad, CA) and grown in RPMI 1640 supplemented with 10% horse serum and 5% fetal bovine serum (all supplies were from Invitrogen). Cells were cultured at 37°C, in the presence of 5% CO_2 and 95% ambient air, and the medium was changed every 2 to 3 days.

CGNs were prepared from 7-day-old Sprague-Dawley rats. Rats were euthanized after carbon dioxide inhalation (anesthesia to minimize pain and discomfort), and cerebellar brain tissue was harvested in accordance with Animal Welfare Act and National Institutes of Health guidelines. The methods used have been described previously (New et al., 1998). In brief, cerebellum was collected, washed, and separated into a single-cell suspension using gentle trypsinization, trituration with a polished glass pipette, and filtration through nylon mesh. After Percoll density gradient centrifugation to remove glia, the neurons were collected and washed twice in sterile medium without serum, then resuspended in Dulbecco's modified Eagle's medium/F-12 medium with 10% horse serum (Invitrogen). Cells were then plated on poly(L-lysine) (70K-150K MW; Sigma Chemical Co., St. Louis, MO)-coated 100-mm culture dishes at a density of 5×10^5 cells/well. One day later, 5-fluorodeoxyuridine (20 mg/ml) and uridine (50 mg/ml) were added to eliminate proliferative cells (astrocytes); the purity of the neuronal population was verified (after 5 days in culture) by immunocytochemical staining for microtubule-associated protein-2. Under these conditions, the cultures were >95% homogeneous for neurons. Neurons were cultured for ≤7 days at 37°C in a humidified atmosphere containing 5% CO_2 and suspended in serum-free Dulbecco's modified Eagle's medium/F-12 for 12 h before the treatments.

Embryonic cortical neurons were kindly provided by Dr. Gregory Brewer (Southern Illinois University, School of Medicine). In brief, neurons were isolated from Sprague-Dawley rat embryos at day 18 of gestation (Brewer et al., 1993). Cortical tissue was dissected, triturated in Hanks' balanced salt solution and centrifuged for 1 min at 11,000*g*. Cells were plated in B27/Neurobasal E (Invitrogen)/glutamine/25 μM glutamate medium on 12-mm diameter glass coverslips (Assistant Brand; Carolina Biologicals, Burlington, NC) coated with poly(D-lysine) at a density of 64,000 cells/cm^2. After 2 weeks of plating, embryonic neurons were treated with 25 μM *S*-nitroso-*N*-acetylpenicillamine (SNAP) and/or 100 μM NO scavenger 2-(4-carboxyphenyl)-4,4,5,5-tetramethylimidazoline-1-oxyl-3-oxide (C-PTIO) for 24 h.

Preparation of Crude Particulate Fraction. Cells were detached in ice-cold phosphate-buffered saline containing 5 mM EDTA, lysed in 10 mM Tris-HCl buffer, pH 7.4, containing 5 mM EDTA, with protease inhibitors, and homogenized with a Polytron homogenizer (Brinkmann Instruments, Westbury, NY). Membranes were obtained by differential centrifugation of the homogenates at 1000*g* for 10 min, followed by centrifugation of the supernatant at 100,000*g* for 15 min. Pellets were resuspended in 50 mM Tris-HCl buffer, pH 7.4, containing 10 mM $MgCl_2$ and 1 mM EDTA. Endogenously released adenosine was degraded using adenosine deaminase (5 U/ml) (Roche Diagnostics, Indianapolis, IN). This mixture was then used for radioligand binding.

Radioligand Binding. Quantification of A_1AR was performed using the antagonist [^{3}H]8-cyclopentyl-1,3-di[2′,3′-3H] propylxanthine (DPCPX) (160 Ci/mmol) purchased from PerkinElmer Life and Analytical Sciences (Waltham, MA). Membrane preparations (50–75 μg of protein) were incubated with the radioligand in the absence or presence of 1 mM theophylline to define nonspecific binding for 1 h at 37°C. The total volume in each assay tube was 250 μl. The reaction mixture was then filtered over polyethylenimine-treated (0.3%) Whatman GF/B glass fiber filters (Brandel Inc., Gaithersburg, MD) and washed with 10 ml of ice-cold Tris buffer containing 0.01% CHAPS. The radioactive content of each filter was determined using a Beckmann liquid scintillation counter (LS5801; Beckman Coulter, Fullerton, CA). Saturation binding data were analyzed using GraphPad Prism (GraphPad Software, Inc., San Diego, CA).

Transfection, Infection, and Luciferase Assay. Cells were grown to approximately 40% confluence and cotransfected with 100 to 250 ng of plasmid vector containing A_1AR promoter coupled to the firefly luciferase reporter gene pBLPniF/PmtA (Ren and Stiles, 1995) or a plasmid vector encoding β-galactosidase, 500–650 ng of carrier DNA, and 3 ml/g DNA of *N*-[1-(2,3-dioleoyloxy)propyl-*N*,*N*,*N*-trimethylammonium methylsulfate (lipofectin) in 50 ml of Opti-MEM (GIBCO BRL). The mixtures were incubated for 45 to 60 min at room temperature before being added to the culture plates. After transfection, cells were grown for another 24 to 36 h. Cells were then lysed using 50 μl of reporter lysis buffer (Promega, Madison, WI) and centrifuged at 4°C at 12,000*g*. Twenty microliters of cell extract

(supernatant) were mixed with 100 μl of luciferase assay reagent (Promega) at room temperature, and the chemiluminescent signal was determined in a luminometer using 1-min counts.

For inhibition of NF-κB, cells were infected with either empty adenovirus vector or a recombinant adenoviral vector containing the mutant form of IκB-α (in which serines at positions 32 and 36 were substituted with alanine) (mIκB-α) and tagged with green fluorescent protein. This vector was kindly provided by Dr. E. M. Schwarz (University of Rochester Medical Center, Rochester, NY). Cells were infected with these vectors (40,000 units) for 24 h, and efficiency of infection was determined by visualizing green fluorescent protein using confocal microscopy. Empty vector-infected cells or cells infected with mIκB-α were treated with either vehicle or Tat (100 nM) for 24 h and then used for radioligand binding studies.

SDS-Polyacrylamide Gel Electrophoresis/Western Blotting. Cell cytosol (50–75 μg) was used for performing SDS-polyacrylamide gel electrophoresis. Proteins were transferred to nitrocellulose membranes, blocked in Blotto buffer (130 mM NaCl, 2.7 mM KCl, 1.8 mM Na_2HPO_4, 1.5 mM KH_2PO_4, 0.1% NaN_3, 0.1% Triton X-100, and 5% nonfat milk) for 2 h and then incubated with the primary antibody at 4°C overnight. All polyclonal antibodies were obtained from Santa Cruz Biotechnology (Santa Cruz, CA). After five washes in blocking solution, blots were incubated with horseradish peroxidase-labeled IgG (GE Healthcare, Chalfont St. Giles, Buckinghamshire, UK) for 1 h at room temperature, washed five times, treated with Western blotting detection reagents (ECL Plus) obtained from Amersham Pharmacia Biotech, and exposed to Kodak XAR film at room temperature (Eastman Kodak, Rochester, NY). Quantification of the gels was performed using software Scion Image Beta 4.02 (Scion Corporation, Frederick, MD).

Immunocytochemistry. PC12 cells were cultured and treated as described in the figure legends. After specific treatments, cultures were washed twice with warm phosphate-buffered saline and fixed with 4% paraformaldehyde for 10 min. After two more washes with phosphate-buffered saline, nonspecific binding was reduced by exposing coverslips for 5 min with a solution containing 5% normal donkey serum and 0.05% Triton X-100. The cells were treated with primary antibody (monoclonal for A_1AR, polyclonal for iNOS), diluted 1:100 in 5% normal donkey serum along with 0.05% Triton X-100 in PBS, and incubated overnight at 4°C. After rinsing four times in phosphate-buffered saline, cells were treated for 1 h with donkey anti-mouse or anti-rabbit IgG labeled with rhodamine (Jackson Immunochemicals, West Grove, PA) diluted 1:200 in 5% normal donkey serum/0.05% Triton X-100 in PBS. After four rinses with phosphate-buffered saline, the coverslips were mounted on glass microscope slides using Aquamount. The cells were observed for red color on an Olympus confocal microscope using Krypton (568 nm) laser and a 20× objective (Olympus, Tokyo, Japan).

Reverse Transcription-Polymerase Chain Reaction (RT-PCR). Total RNA was prepared using the guanidinium isothiocyanate method. Total RNA (5–10 μg each) was reverse-transcribed using first-strand cDNA synthesis kit (Pharmacia LKB Biotechnology, Inc., Uppsala, Sweden) in a total volume of 15 μl. The first-strand mix (0.25–0.5 μl) was then used for PCR amplification. Primers used included sequences 5′-GCCTCGCTCTGGAAAGA-3′ (sense) and 5′-TCCATGCAGACAACCTT-3′ (antisense) for iNOS, 5′-TGAAGGTCGGTGTCAACGGATTTGGC-3′ (sense) and 5′- CATGTAGGCCATGAGGT CCACCAC-3′ (antisense) for glyceraldehyde 3-phosphate dehydrogenase (GAPDH), and 5′-CATCCCACTGGCCATCCTTAT-3′ (sense) and 5′-AGGTATCGATCCACAGCA-3′ (antisense) for rat A_1AR. PCR generated a 477-bp fragment of iNOS, a 983-bp fragment of GAPDH, and a 115-bp fragment for the A_1AR. PCR reactions were performed in a total volume of 50 μl containing 2.5 mM $MgCl_2$. The sequences of interest were amplified over 27 to 36 cycles. The amplified products were resolved on 1.2 to 2% agarose gels and visualized by ethidium bromide staining.

Electrophoretic Mobility Shift Assay. Nuclear extracts were prepared from cells as described previously (Pingle et al., 2003). EMSAs were performed by incubating nuclear extracts with ^{32}P-labeled double-stranded oligonucleotide probes in reaction buffer as described previously (Pingle et al., 2003). Protein-DNA complexes were resolved using 4% nondenaturing polyacrylamide gels that, after drying, were exposed to X-ray films (GE Healthcare, Chalfont St. Giles, Buckinghamshire, UK). The fold increase in the expression of the transcription factors was determined using background subtract. The probes used in these assays were as follows: NF-κB, 5′-CAACGGCAGGGGAATTCCCCTCTCCTT-3′; activator protein-1 (AP-1), 5′-TGTCGAATGCAAATCACTAGAA-3′; and OCT-1, 5′-TGTCGAATGCA AATCACTAG AA-3′.

Apoptosis Detection. Apoptosis was detected using either annexin V-FITC apoptosis kit (Oncogene Research Products, San Diego, CA) or by terminal deoxynucleotidyl transferase-mediated digoxigenin-dUTP nick end-labeling (TUNEL) assay. Annexin V-FITC assays were performed according to the manufacturer's recommendations and analyzed by flow cytometry using FACS Calibur Cytometer (BD Biosciences, Mountain View, CA) equipped with argon ion laser light source emitting an excitation light at 488 nm, leading to high FITC emission, and a 530/30 bandpass filter that transmits wavelengths of light between 515 and 545 nm.

For detecting apoptosis in PC12 cells, CGNs, and cortical neurons, apoptotic cells were visualized using TUNEL assay, according to the manufacturer's instructions (Intergen Co., Purchase, NY). In brief, the cells were treated with Tat 1–72 (100–500 nM) or SNAP (25 μM) in the presence of other reagents for 24 to 72 h. After the treatments, the cells were washed with ice-cold PBS, fixed with 4% paraformaldehyde, and then placed in equilibrating buffer and incubated in a reaction buffer containing TdT and dUTP for 60 min at 37°C. After rinsing, the cells were incubated with peroxidase-conjugated anti-digoxigenin (introduced together with Triton X-100 and a blocking agent). The cells were then exposed to 0.5 mg/ml diaminobenzidine and 0.05% hydrogen peroxide to generate a brown reaction product. The percentage of TUNEL-positive cells (brown) was assessed by analysis of digitized images from 12 or more microscopic fields of TUNEL-stained cells from tag-image file format files (Adobe Photoshop version 7.0; Adobe Systems, Mountain View, CA).

Assay for Nitric-Oxide Production. Intracellular nitric-oxide production was detected using 4,5-diaminofluorescein diacetate (DAF-2 DA) (Calbiochem, San Diego CA). Cells were grown on poly(D-lysine)-coated coverslips, treated with the indicated drugs, washed with PBS, and then loaded with 5 μM DAF-2 DA for 20 min at 37°C. After washing with 1× PBS, cells were imaged for green fluorescence 30 min later using an Olympus Fluoview confocal laser-scanning microscope argon laser (488 nm wavelength) and a 20× objective.

Ca^{2+} Imaging. Cells were grown on glass coverslips, washed with normal extracellular solution (140 mM NaCl, 4 mM KCl, 10 mM HEPES, 5 mM glucose, 2 mM $CaCl_2$, and 2 mM $MgCl_2$ at pH 7.4) and loaded with the calcium indicator dye Fluo-4 AM (Invitrogen) at a concentration of 5 μM. After incubation at room temperature for 30 to 45 min, the cells were washed with extracellular solution and imaged with an argon laser at 488 nm. Images were recorded at baseline (F_0), and the image was scanned over time (F) as the indicated compounds were added to the cells at optimal time points. Further analysis of the image obtained was carried out using the Olympus Fluoview software.

Protein Determination and Statistical Analyses. The level of protein in samples was determined by the established method (Bradford, 1976), using bovine serum albumin to prepare standard curves. Statistical analyses for radioligand binding was done using GraphPad Prism. Other statistical analyses were done using Student's t test and analysis of variance.

Results

Demonstration of A_1AR Expression in PC12 Cells. The expression of A_1AR in PC12 cells has not been shown

previously. These cells were used previously primarily as a model for the A_{2A}AR (Guroff et al., 1981; Nie et al., 1999). Hence, initial experiments were performed to determine whether these cells also express the A_1AR. Radioligand binding experiments using increasing concentrations of the antagonist radioligand [^{3}H]DPCPX revealed saturable binding, with maximum binding sites (B_{max}) being 40 ± 6 fmol/mg protein and an equilibrium dissociation constant (K_d) of 4.4 ± 1.3 nM (Fig. 1, A and B). Likewise, identification of the A_1AR was obtained using the agonist radioligand [^{125}I]4-aminobenzyl-5′*N*-methylcarboxamido adenosine (data not shown). Surface expression of A_1AR was confirmed by immunocytochemistry using a monoclonal antibody for this receptor (Ochiishi et al., 1999) and a rhodamine-conjugated secondary antibody (Fig. 1C), in which A_1AR appeared as red fluorescence localized to the outer rim of the cell. Under similar incubation conditions, no immunolabeling was detected in cells treated with preimmune serum. In addition, we measured the A_1AR transcripts using RT-PCR (Fig. 1D). The predicted 115-bp PCR product obtained after 36 amplification cycles was visualized on a 1.8% agarose gel using ethidium bromide staining.

Activation of the A_1AR Suppresses HIV-1 Tat-Induced Increase in $[Ca^{2+}]_i$ Release. Previous studies have indicated that HIV-1 Tat significantly increases $[Ca^{2+}]_i$ levels, which triggers apoptotic cell death (Haughey et al., 1999). We examined whether A_1AR activation alters Tat-induced increase in $[Ca^{2+}]_i$ in PC12 cells. Both 50 nM (data not shown) and 100 nM HIV-1 Tat increased $[Ca^{2+}]_i$ release. The administration of 100 nM Tat produced a rapid increase in $[Ca^{2+}]_i$ levels, observed within 5 s (Fig. 2A). This increase in $[Ca^{2+}]_i$ release was transient and returned to baseline rapidly (<1 min). Pretreatment of cells with 1 μM *R*-phenylisopropyladenosine (R-PIA) produced a substantial reduction in the maximal Tat-mediated $[Ca^{2+}]_i$ release by ~85% (Fig. 2, B and C).

Additional experiments were conducted to determine the AR subtype(s) involved in the suppression of $[Ca^{2+}]_i$ release by R-PIA. For these experiments, cells were pretreated with either A_1AR-specific antagonist DPCPX (1 μM), A_{2A}AR-specific antagonist ZM241385 (1 μM), or A_3AR-specific antagonist MRS1220 (1 μM), 30 min before the addition of 1 μM R-PIA and/or 100 nM HIV-1 Tat (Fig. 2C). We observed reversal of the agonist response with DPCPX, whereas ZM241385 and MRS1220 did not affect the Ca^{2+} response. These data strongly suggest a predominant role of the A_1AR in attenuating Tat-induced $[Ca^{2+}]_i$ release.

To determine the source of Ca^{2+} release subsequent to Tat application, PC12 cells were imaged in Ca^{2+}-free extracellular solution with 5 mM EGTA. We observed a small but insignificant diminution of the Tat response (Fig. 2D), suggesting that the source of Ca^{2+} released in response to Tat application is not from extracellular sources. Depletion of $[Ca^{2+}]_i$ using 10 μM thapsigargin inhibited Tat-mediated increase in $[Ca^{2+}]_i$ release (Fig. 2D), suggesting that internal stores are the likely source of Ca^{2+} release as determined previously (Haughey et al., 1999). Furthermore, pretreatment of cells with 100 ng/ml pertussis toxin for 4 h reduced the increase in $[Ca^{2+}]_i$ release (Fig. 2D), implicating a pertussis toxin-sensitive G-protein in mediating this response in PC12 cells, as reported previously (Haughey et al., 1999). These data implicate an intracellular source of Ca^{2+} accessible to Tat, which is specifically inhibited by A_1AR activation. Because the concentrations of R-PIA and DPCPX used could also interact with other AR subtypes, we performed experiments using lower concentrations of both of these agents on Tat-mediated intracellular Ca^{2+} release. As shown in Fig. 2E, inhibition of the Tat response was evident at the lowest concentration of R-PIA tested (1 nM), and the extent of inhibition was greater with increasing concentrations of the agonist, with maximal response obtained at 100 nM R-PIA. Likewise, we observed reversal of the R-PIA (1 μM) inhibition using 50 and 100 nM DPCPX. These data would further support an involvement of the A_1AR in mediating the response to these AR analogs.

A_1AR Activation Attenuates HIV-1 Tat-Induced NO Production and iNOS Expression. It is well known that an increase in $[Ca^{2+}]_i$ can activate the constitutive isoform of the enzyme nitric oxide synthase (Moncada et al., 1991), which in turn leads to production of nitric oxide (NO). In addition, Ca^{2+}-induced NF-κB activation can also up-regulate the expression of the inducible isoform of this enzyme (iNOS) (Chen et al., 2005). Hence, in the next set of experiments, we determined whether Tat promotes NO release

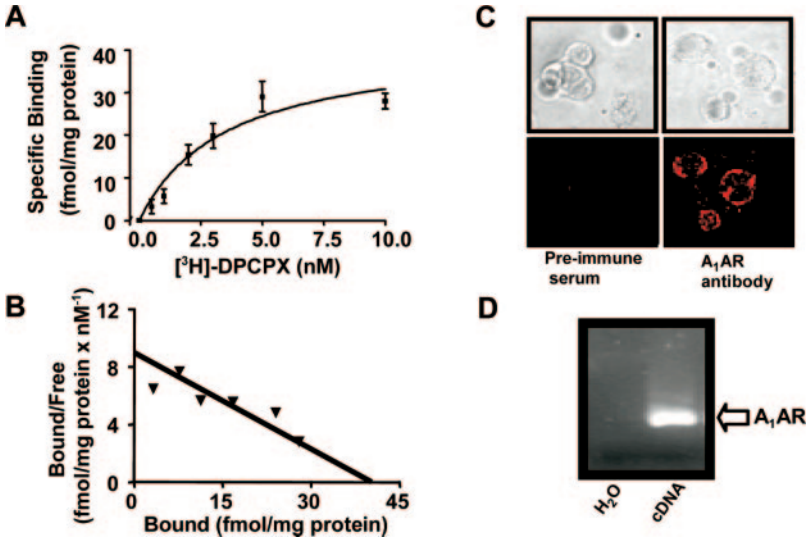

Fig. 1. Demonstration of adenosine A_1 receptor in PC12 cells. Radioligand binding experiments were carried out using approximately 80 μg of membrane protein per assay tube. A, saturation curves using increasing concentration of [^{3}H]DPCPX demonstrates a saturable binding with a B_{max} of 40.3 ± 6 fmol/mg protein and a K_d of 4.4 ± 1.3 nM. Data were analyzed by GraphPad Prism and were best-fitted using a single-site fit. B, Scatchard plot of saturation data presented in A. C, demonstration of A_1AR in PC12 cells by immunocytochemistry. Cells were incubated with preimmune serum (left) or monoclonal antibody (right) for the A_1AR, followed by rhodamine-tagged goat anti-mouse IgG as secondary antibody. Cells were visualized by confocal microscopy using Krypton laser at 200× magnification. D, identification of the A_1AR transcript by RT-PCR. Total RNA was reverse-transcribed and amplified using sense and antisense primers for 36 cycles. Product was resolved on a 1.5% agarose gel and visualized by ethidium bromide staining. The data are representative of at least three independent experiments.

from PC12 cells. Cells treated with 100 nM HIV-1 Tat for 6 h demonstrated a significant increase in NO release, which was attenuated by pretreatment of these cells with 1 μM R-PIA 30 min before the addition of Tat (Fig. 3, A and B). Furthermore, this effect of R-PIA was significantly reversed by incubation of cells with the A_1AR-specific antagonist DPCPX (1 μM) ($p < 0.05$, compared with Tat + R-PIA treatment), suggesting a role of A_1ARs in the inhibition by R-PIA.

Previous studies have demonstrated that HIV-1 Tat increases iNOS in neuronal cells, the NO derived from which is implicated in neuronal damage produced by its conversion to peroxynitrite (Kruman et al., 1998). We speculated that A_1AR activation could negate this response of Tat and thereby confer cytoprotection. The levels of iNOS were determined by Western blotting and immunocytochemistry after 18 h of treatment. The iNOS protein was detected as a predominant 130-kDa protein on Western blot and showed a mobility similar to that of the purified mouse protein, used as a positive control (data not shown). Minor immunoreactive bands were also identified below 130 kDa, which might represent iNOS degradation products. Cells exposed to Tat showed a significant increase (2-fold) in iNOS expression (quantitating only the 130-kDa band), compared with control cells treated with vehicle (Fig. 3C). To test the effect of A_1AR activation on iNOS expression, PC12 cells were pretreated with R-PIA (1 μM) 30 min before the addition of HIV-1 Tat (100 nM) for 18 h. Pretreatment with R-PIA (1 μM) almost completely abolished the induction of iNOS by Tat, which was partially reversed by A_1AR blockade using DPCPX (1 μM). The addition of R-PIA did not affect the basal level of iNOS protein (Fig. 3D). The relative levels of iNOS in control, R-PIA-treated, and Tat-treated cells were 100, 86, and 166, respectively (mean of two experiments).

The suppression of iNOS induction by R-PIA observed by Western blotting was confirmed by immunocytochemistry. Immunoreactivity for iNOS appeared as a reddish-orange cytoplasmic stain, surrounding the yellow-green nuclear staining provided by Sytox (for staining the nucleus). Cells exposed to Tat showed substantially elevated expression of iNOS (detected as yellow to reddish-orange cellular fluorescence) compared with untreated controls (yellow-green fluorescence), whereas pretreatment with R-PIA attenuated this

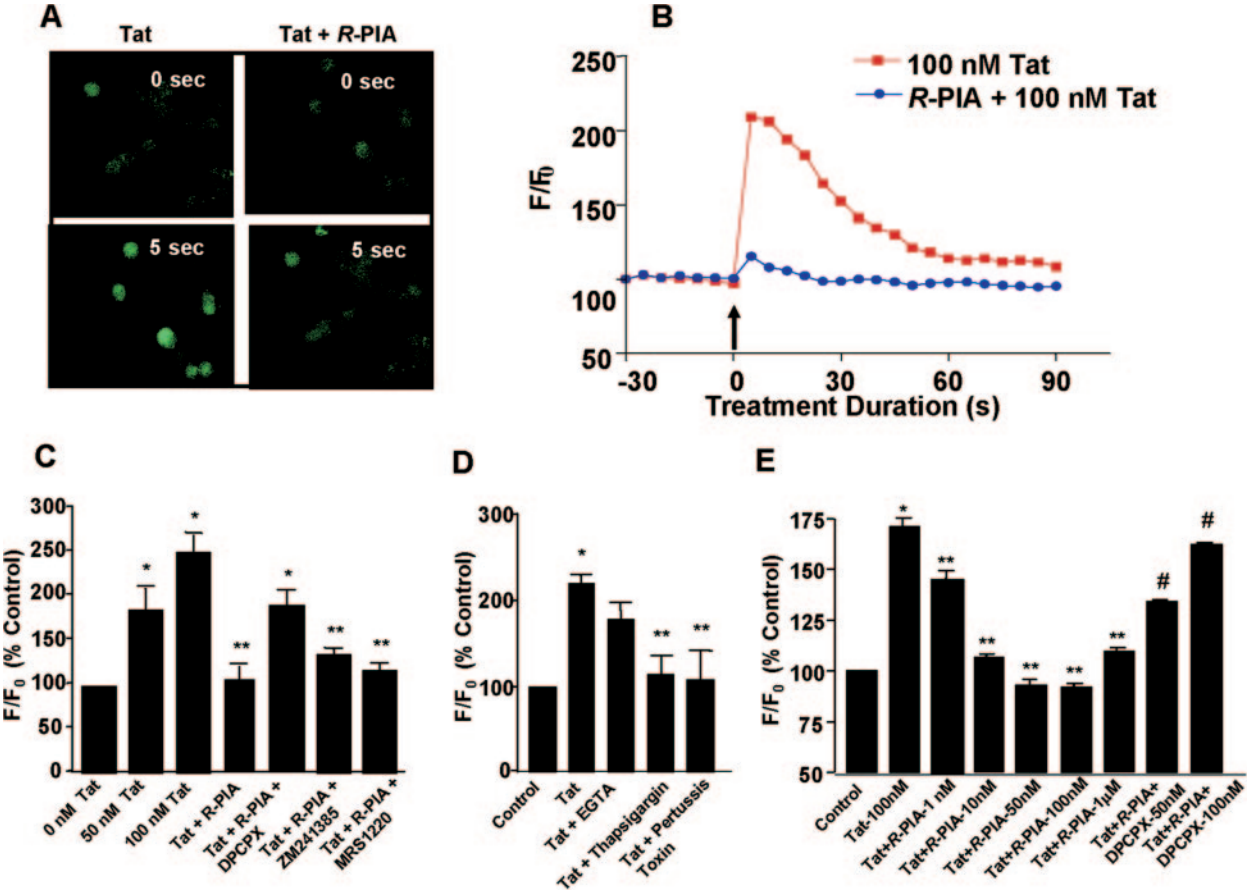

Fig. 2. A_1AR inhibits Tat-induced increase in intracellular Ca^{2+} release. For Ca^{2+}-imaging studies, PC12 cells were grown on coverslips and loaded with the 5 μM Fluo-4 AM. Cells were then visualized under a confocal microscope using an argon laser (488 nm). A and B, treatment with 100 nM Tat induced a rapid (within 5 s) increase in intracellular Ca^{2+}, which returned to the basal level in ~60 s. Pretreatment of cells with the adenosine analog R-PIA (1 μM) attenuated this increase in intracellular Ca^{2+} release by 85%. Arrow in B indicates the time point of treatment. C, inhibition of 100 nM Tat-induced intracellular Ca^{2+} release by R-PIA was reversed by the selective A_1AR antagonist DPCPX ($p < 0.05$) but not by selective inhibitors of the A_{2A}AR (ZM241385) or the A_3AR (MRS1220). D, chelation of extracellular Ca^{2+} by EGTA or depletion of $[Ca^{2+}]_i$ release by thapsigargin attenuated Tat-induced increase in $[Ca^{2+}]_i$ release. Pertussis toxin treatment (100 ng/ml, 24 h) also inhibited Tat-induced $[Ca^{2+}]_i$ release. E, inhibition of Tat-mediated intracellular Ca^{2+} release by R-PIA and attenuation by DPCPX. Cells were pretreated with different concentrations of R-PIA or a combination of R-PIA (1 μM) and different concentrations of DPCPX for 30 min followed by Tat (100 nM), and Ca^{2+} imaging was performed immediately by confocal microscopy, and fluorescence was plotted over baseline values. *, statistically significant difference ($p < 0.05$) from control; **, statistically significant difference from Tat-treated groups; #, statistically significant difference from R-PIA + Tat-treated group ($p < 0.05$). The data are representative of at least three independent experiments.

induction (Fig. 3E). To determine whether the changes in iNOS expression were associated with concomitant changes in iNOS RNA, the steady-state levels of mRNA were determined by RT-PCR. The product obtained by PCR was ~477 base pairs in length, as predicted from the primers used, and mRNA levels were normalized to levels of GAPDH RNA (Fig. 3F). Quantitation of these changes showed that exposure to HIV-1 Tat for 12 h produced a 2.5 ± 0.2-fold increase in iNOS mRNA, which was attenuated in cells pretreated with 1 μM R-PIA. In this latter group, the induction by HIV-Tat was 1.4 ± 0.1-fold. Addition of DPCPX (1 μM) reversed the effect of R-PIA (statistically significant change from R-PIA, $p < 0.05$), indicative of a role of the A_1AR in mediating this response (Fig. 3F).

To determine whether the inhibition of iNOS expression by A_1AR could be related to this receptor inhibition of HIV-Tat-dependent $[Ca^{2+}]_i$ release, cells were pretreated with or without (control) 20 μM BAPTA-AM before administration of Tat (100 nM). As observed previously, Tat increased iNOS expression by 1.4 ± 0.1-fold in control cells but not in cells pretreated with BAPTA-AM, in which the change was 0.9 ± 0.2-fold (Fig. 3G). These data suggest that inhibition of intracellular Ca^{2+} release could explain the inhibition of Tat-induced iNOS expression via the A_1AR.

A_1AR Activation Suppresses Tat-Induced Activation of NF-κB. To determine the mechanism underlying the inhibition of Tat-induced expression of iNOS, we examined the activity of transcription factors known to regulate the level of this protein. In this regard, the principal focus was on NF-κB, which is an important target for HIV-1 Tat (Conant et al.,

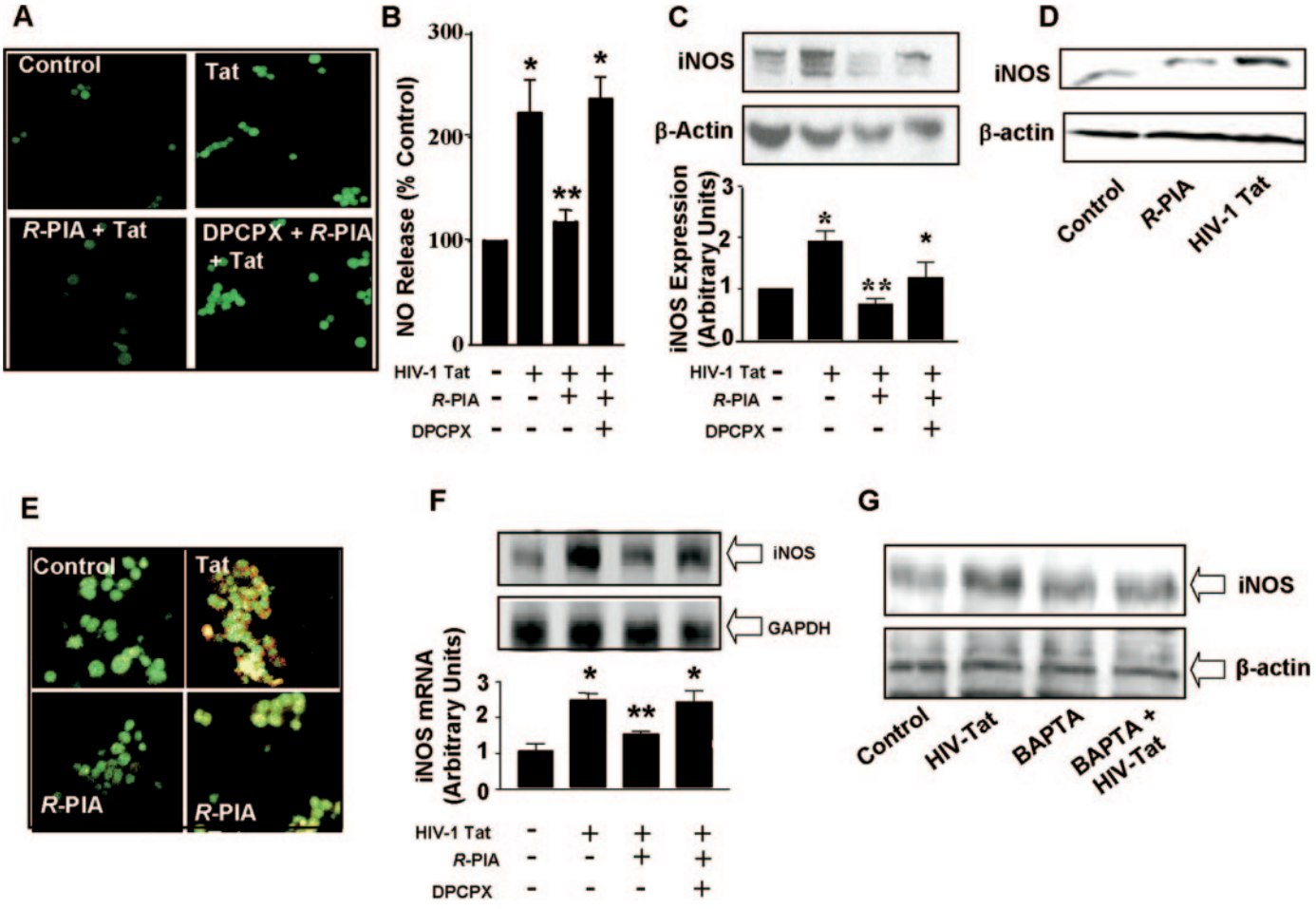

Fig. 3. A_1AR inhibits Tat-induced iNOS expression. PC12 cells were exposed to HIV-1 Tat (100 nM) for 24 h, with or without 1 μM R-PIA or R-PIA and/or 1 μM DPCPX. Control cells were treated for the same period of time with vehicle (1 mg/ml bovine serum albumin + 0.1 mM dithiothreitol). A, Tat increases NO release is blocked by A_1AR activation. Cells were treated with either vehicle, or R-PIA (1 μM) and/or DPCPX for 30 min, followed by the addition of vehicle or HIV-1 Tat (100 nM) for 18 h. NO release was measured by confocal microscopy using the indicator DAF-2 DA (5 μM) with wavelength setting of 488 nm. B, quantitation of the NO release data from A. The data are representative of three separate experiments. C, cells were then lysed, and extracts (50 μg of protein per lane) were used in Western blotting assays for iNOS. Blots were normalized to β-actin levels, and the results are depicted in histograms. Data are expressed as the mean ± S.E. of four independent experiments. D, R-PIA did not alter basal iNOS levels. The treatments were for 24 h, and the relative iNOS levels for control, R-PIA, and Tat treatments averaged 100, 86, and 166 (mean of two experiments). E, immunocytochemistry was performed using a polyclonal antibody against iNOS as the primary antibody and a rhodamine-tagged secondary antibody. Nuclear staining was performed using Sytox and was visualized as bright yellow fluorescence. Visualization of the labeled proteins (red) was performed using confocal microscopy with a 200-fold magnification. F, PC12 cells were treated similarly for 12 h, total RNA was extracted, reverse-transcribed, and used for PCR utilizing specific primers for iNOS and GAPDH. The PCR products were resolved using 1.2% agarose gels. The band intensities were quantitated by densitometry, and iNOS band was normalized to GAPDH mRNA. The data shown is representative of three separate experiments. *, statistically significant difference from control cells ($p < 0.05$); **, statistically significant difference from Tat-treated cells ($p < 0.05$). G, inhibition of intracellular Ca^{2+} by BAPTA-AM (20 μM) inhibits HIV-Tat induced iNOS expression. The data are representative of three independent experiments showing similar findings. Note that the effects of DPCPX + R-PIA in B, C, and F were statistically significant ($p < 0.05$) from those obtained with R-PIA alone.

1996). PC12 cells were treated with HIV-1 Tat (50 or 100 nM) for 30 min, and nuclear fractions were isolated and used to perform EMSAs. We observed a significant increase in the nuclear NF-κB DNA binding activity to the radiolabeled oligonucleotide, which contains the cis-acting NF-κB-responsive element (Fig. 4A). Pretreatment of cells with 1 μM R-PIA for 15 min resulted in a dramatic reduction in the activation of NF-κB by Tat at both doses tested. Bands obtained were normalized to Oct-1 transcription factor (Fig. 4A).

We next examined whether the AP-1 transcription factor is also a target for inhibition by A_1AR activation. Previous studies have shown that Tat activates this transcription factor in human histiocytic lymphoma U937 cells (Kumar et al., 1998). Using EMSAs, we observed activation of AP-1 by Tat. However, unlike NF-κB, AP-1 activation was not inhibited but instead was activated by A_1AR stimulation (Fig. 4B). This observation could be explained by A_1AR activation of the extracellular signal-regulated kinase 1/2 pathway (Faure et al., 1994; Robinson and Dickenson, 2001; Jajoo et al., 2006) and possible downstream activation of AP-1 transcription factor. As such, inhibition of the A_1AR by DPCPX led to inhibition of the receptor activation of AP-1 (Fig. 4B). After a similar treatment protocol, we observed no activation by Tat of cAMP response element binding protein and CCAAT/enhancer-binding protein-β (data not shown).

HIV-1 Tat Induces Expression of the A_1AR. Because the A_1AR is known to be regulated by NF-κB, we next determined whether HIV-1 Tat induces its expression in PC12 cells. Receptor binding studies, using a single concentration of the antagonist radioligand [^{3}H]DPCPX (~1 nM), have shown the levels of A_1AR in controls to be 5.7 ± 1.3 fmol/mg protein and 9.7 ± 1.4 fmol/mg (70 ± 25% increase, $p < 0.05$) after 24-h treatment with 100 nM Tat (Fig. 4C). To test whether this effect of Tat is mediated by de novo transcription of the A_1AR gene, the ability of Tat to increase A_1AR gene promoter activity in PC12 cells transiently transfected with pBLPnif/PmtA (Ren and Stiles, 1995) was examined. A 2- to 3-fold increase in luciferase activity was observed when these cells were treated with 100 nM Tat for 24 h (Fig. 4D). Luciferase activity was normalized to β-galactosidase activity. To determine whether NF-κB is involved in the induction of the A_1AR by Tat, PC12 cells were infected with an adenoviral vector expressing a mutant form of IκB-α (mIκB-α) that acts as a super-repressor of NF-κB (Pingle et al., 2003). EMSAs using extracts from PC12 cells expressing mIκB-α demonstrated decreased NF-κB binding to its oligonucleotide compared with control (data not shown), indicating that mIκB-α inhibited NF-κB activity. In addition, we determined A_1AR levels using radioligand binding and observed that in control cells, HIV-1 Tat induced a 65 ± 10% increase in number of A_1AR, whereas in cells expressing mIκB-α, Tat did not show any significant increase in A_1AR (6 ± 7% increase compared with control; Fig. 4E).

A_1AR Activation Protects PC12 Cells against HIV-1 Tat-Induced Apoptosis. The observation that A_1AR activation reduces Tat-mediated increases in $[Ca^{2+}]_i$, iNOS ex-

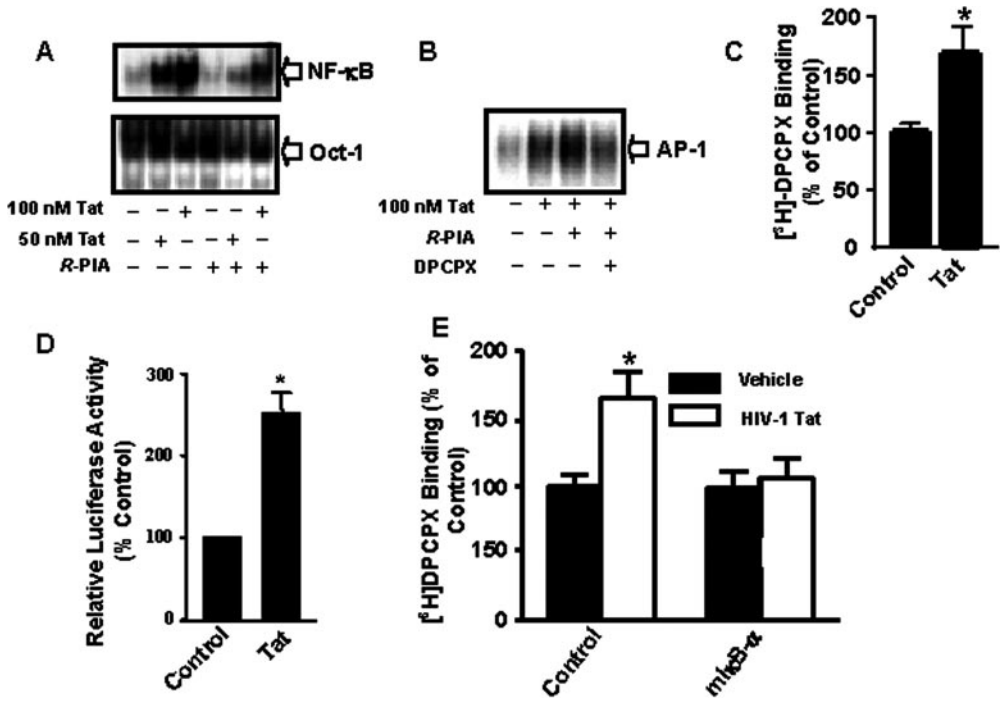

Fig. 4. Inhibition of Tat-induced activation of NF-κB by A_1AR and Tat induction of A_1AR. A, PC12 cells were pretreated with either vehicle or R-PIA for 30 min followed by the addition of 50 or 100 nM HIV-1 Tat. Nuclear extracts were prepared, and EMSAs were performed using ^{32}P-labeled consensus oligonucleotide sequence for NF-κB. The same nuclear extracts were examined for Oct-1 binding for normalization. B, EMSA using ^{32}P-labeled oligonucleotide for AP-1 transcription factor. The data shown are representative of four separate experiments for NF-κB and AP-1. C, Tat-increased the binding of [^{3}H]DPCPX. Cells were exposed to Tat for 24 h, and radioligand binding assays were performed on crude plasma membranes using 1 nM radioligand. HIV-1 Tat increased A_1ARs by ~60% compared with control. D, Tat increased A_1AR promoter activity in PC12 cells were cotransfected with a plasmid vector containing the A_1AR promoter coupled with a firefly luciferase reporter gene (pBLPnif/PmtA) and β-galactosidase using lipofectin. Luciferase activity was determined after the addition of Tat (100 nM) for 20 h and normalized to β-galactosidase activity. E, radioligand binding in control and cells in which NF-κB was repressed with a viral vector encoding mIκB-α and treated with vehicle or HIV-1 Tat (100 nM) for 20 h. Asterisk indicates statistical significance from control. Results are a representative or the mean ± S.E.M. of three to five individual experiments.

pression, and NO release provided the rationale for determining whether receptor activation confers protection against Tat-induced cytotoxicity. PC12 cells were treated with either 50 or 100 nM Tat for 24 h, either alone or after pretreatment with 1 μM R-PIA. HIV-1 Tat produced a significant increase in apoptosis in PC12 cells (see arrows) compared with control (32 $\pm$ 6 and 40 $\pm$ 3% apoptotic cell, using 50 and 100 nM Tat, respectively). Preincubation with R-PIA resulted in a statistically significant reduction in the number of apoptotic cells to 18 $\pm$ 2% (Fig. 5, A and B). The number of apoptotic cells in the absence of any treatment and in the presence of R-PIA alone were 8 $\pm$ 1 and 7 $\pm$ 1%, respectively (Fig. 5, A and B).

Tat-induced apoptosis was confirmed by flow cytometry using an annexin V-FITC kit. The percentage of apoptotic cells in the absence of drug treatment was 4 $\pm$ 3% and increased to 43 $\pm$ 1 after treatment with 100 nM HIV-1 Tat for 24 h. In cells pretreated with R-PIA followed by HIV-1 Tat, the number of apoptotic cells was significantly reduced to 8 $\pm$ 8% compared with HIV-1 Tat-treated cells. It is noteworthy that A_1AR-specific antagonist DPCPX partially reversed this effect of R-PIA (33 $\pm$ 6% apoptotic cells) ($p < 0.05$ compared with R-PIA), indicating a significant involvement of this receptor subtype in the R-PIA effect (Fig. 5, C and D).

Because our data demonstrate the inhibition of iNOS expression and attenuation of Tat-induced apoptosis by A_1AR, we performed additional experiments to determine whether the inhibition of iNOS could account for the cytoprotective effect of the A_1AR. Pretreatment of PC12 cells with 250 μM N^G-nitro-L-arginine methyl ester (L-NAME) provided significant protection against Tat-induced apoptosis (Fig. 6, A and B). Because L-NAME is an inhibitor of NOS, its ability to protect cells implicates NOS as a likely mediator of Tat-induced apoptosis. As such, inhibition of iNOS expression could represent one of the mechanisms by which A_1AR activation protects PC12 cells against Tat toxicity.

Additional studies were performed in primary cultures of embryonic cortical neurons to directly test whether NO could produce apoptosis. Cortical neurons were exposed to vehicle or 20 μM of the NO donor, SNAP, and/or 100 μM of the NO scavenger, C-PTIO, for 24 h, and the percentage of apoptotic cells was determined by TUNEL assays. We observed a statistically significant increase in TUNEL-positive cells from 12 $\pm$ 3% in the controls to 76 $\pm$ 6% ($p < 0.05$) in the SNAP-treated group. Cultures pretreated with C-PTIO before SNAP showed a statistically significant reduction in apoptotic cells compared with the SNAP-treated group ($p < 0.05$). In addition, we observed that the total number of cells per microscope field was also significantly reduced by SNAP and that this reduction was partly reduced by C-PTIO. The cell number per field averaged 351 $\pm$ 15, 188 $\pm$ 16, and 281 $\pm$ 10 for the control, SNAP-treated group, and C-PTIO + SNAP-treated groups, respectively.

A_1AR Activation Modulates Pro- and Antiapoptotic Regulators in Tat-Treated Cells. To further elucidate the downstream mechanism(s) that might be involved in A_1AR-mediated protection, we studied the effect of Tat on members of Bcl-2 family proteins, specifically antiapoptotic Bcl-2 and proapoptotic Bax. PC12 cells were treated with 100 nM HIV-1 Tat for 18 h either alone or in the presence of R-PIA, and DPCPX and cell extracts were analyzed for Bcl-2 and Bax levels by Western blotting. We observed no significant change in Bcl-2 levels after Tat treatment (Fig. 7A). However, HIV-1 Tat produced a ~3-fold induction of Bax. Furthermore, R-PIA pretreatment reduced levels of Bax in Tat-treated cells. In the presence of DPCPX, R-PIA was unable to inhibit Tat-induced up-regulation of Bax (Fig. 7). We also examined levels of the effector caspase, caspase-3, after Tat treatment. Cells treated with Tat (100 nM) for 18 h demonstrated increased caspase-3 expression by ~2-fold, which was inhibited (~40% inhibition) by 1 μM R-PIA. The inhibition of caspase-3 by R-PIA was partially reversed by treatment with

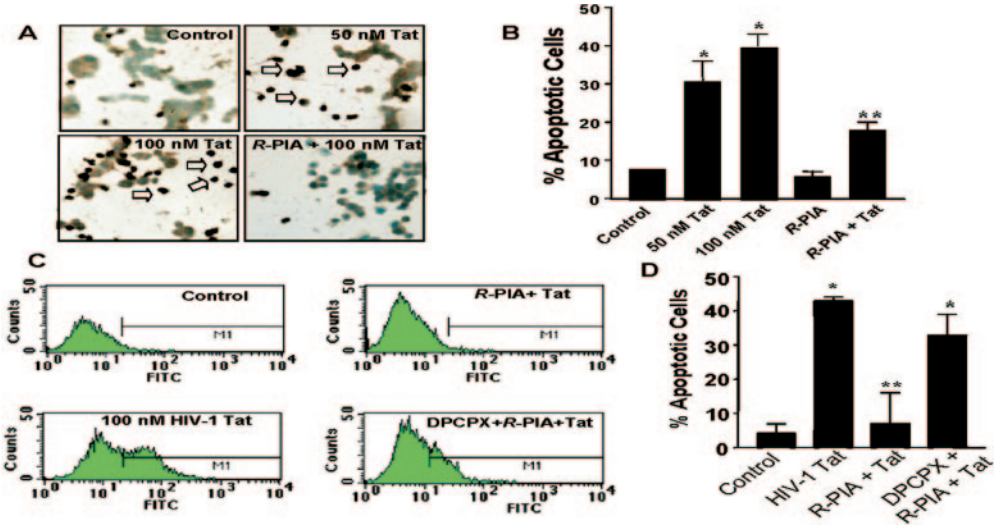

Fig. 5. Activation of A_1ARs protects PC12 cells against Tat-induced apoptosis. PC12 cells were treated with HIV-1 Tat (50 or 100 nM) alone or after pretreatment with 1 μM R-PIA or R-PIA + 1 μM DPCPX, and level of apoptosis was determined by TUNEL assay after 24 h. A, TUNEL-positive (apoptotic) cells appear dark brown to gray-black in color because of diaminobenzidine-stained nuclei (marked with arrow), compared with light brown- or green-stained nuclei in nonapoptotic cells. Percentage of TUNEL-positive cells per 20 high-power fields were averaged and are presented in B. C, apoptosis was also detected by flow cytometry using a fluorescein-conjugated enzyme and 488 nm argon ion laser. Flow cytometric data are represented in a bar graph denoting the intensity of fluorescence. Results are presented as the mean $\pm$ S.E. of apoptotic cells from three independent experiments. *, statistically significant difference from control cells ($p < 0.05$). **, statistically significant difference from Tat-treated cells ($p < 0.05$). The response of Tat + R-PIA + DPCPX was statistically different from that of R-PIA + Tat ($p < 0.05$).

the antagonist DPCPX, implicating the A_1AR in this response (Fig. 7A). Unlike its effect on Tat-mediated increases in proapoptotic proteins, R-PIA did not alter the basal levels of Bax, Bcl-2, or caspase-3 proteins (Fig. 7B).

HIV-Tat Mediated Apoptosis in Cerebellar Granule Cells Is Inhibited by Activation of the A_1AR Agonist and Inhibition of NOS. To determine whether the inhibition of HIV-1 Tat-dependent apoptosis by the A_1AR is observed in primary neuronal cultures, we examined the effect of R-PIA on Tat-dependent apoptosis in CGNs. Cells were treated with or without 500 nM Tat in the absence or presence of adenosine analogs or L-NAME. We observed a significant increase in TUNEL-positive cells (30 ± 3% apoptotic cells) in cultures treated with Tat for 24 h compared with untreated cells (4 ± 2% apoptotic cells) (Fig. 8A). R-PIA significantly reduced the number of apoptotic cells produced by Tat to 7 ± 2%, and this response was reversed by DPCPX, implicating the A_1AR in mediating this response. CGS21680 was ineffective against Tat-mediated apoptosis, suggesting that the A_{2A}AR was probably not involved in mediating this response (Fig. 8A). However, L-NAME effectively inhibited Tat-dependent apoptosis, suggesting a role of NO in mediating the toxicity of Tat. Another interesting observation is that the cell numbers obtained with the different treatment combinations were significantly different after 24 h. For example, we observed reductions in cell number in the Tat, Tat + R-PIA + DPCPX, and the Tat + CGS21680 treatment groups compared with the controls (Fig. 8B). Cell numbers were not statistically different in the control, Tat + R-PIA, and Tat + L-NAME treatment groups.

Additional experiments were performed to determine whether the protective effects of R-PIA and L-NAME could be maintained over a 72-h period in cultures treated in a similar fashion as described above. Results obtained from these studies indicate a more pronounced protective action induced by these two agents. Tat induced a significant increase in cell loss (70 ± 2%) after 72 h, which was reduced to 9 ± 1% by coadministering Tat with R-PIA and to 4 ± 1% by coadministering Tat with L-NAME (Fig. 8C). As observed at 24 h, DPCPX reversed the protective effect of R-PIA ($p < 0.05$), whereas CGS21680 was devoid of any protective effect. An effect on cell number, similar to that observed at 24 h, was also evident. Both R-PIA and L-NAME treatments significantly reduced the loss in cell number compared with cells treated with Tat, Tat + R-PIA + DPCPX, and Tat + CGS21680 (Fig. 8D).

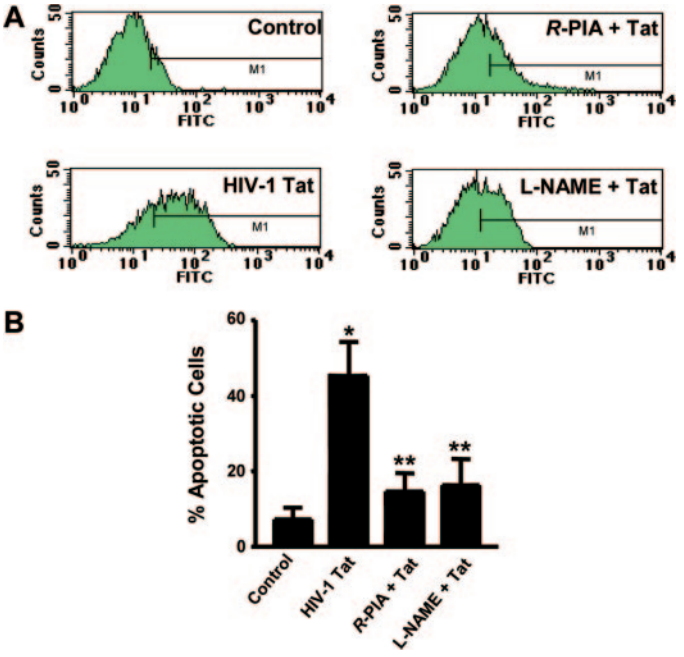

Fig. 6. Inhibition of nitric-oxide synthase protects PC-12 cells from Tat-induced apoptosis. A, PC12 cells were treated for 24 h with 100 nM Tat alone or in the presence of 1 μM R-PIA or 250 μM L-NAME and examined for apoptosis by flow cytometry. B, results are presented as mean ± S.E. of the percentage of apoptotic cells. Results are the mean ± S.E. of three independent experiments. *, statistically significant difference from control cells ($p < 0.05$). **, statistically significant difference from Tat-treated cells ($p < 0.05$).

Discussion

Several studies have identified HIV-1 Tat as an important mediator of HIV encephalitis (Jones et al., 1998; Kaul et al., 2001). Tat is secreted from HIV-1-infected glia and macrophages to adversely influence neuronal function. Because the A_1AR is the prime target of adenosine to mediate cytoprotection in the central nervous system (Ramkumar et al., 2001), we focused on this AR subtype as a target for mediating protection against Tat-induced apoptosis in vitro. Our results demonstrate that A_1AR protects against Tat-mediated apoptosis by attenuating the increase in intracellular Ca^{2+} and subsequent NOS activity/expression.

An increase in intracellular Ca^{2+} via the phospholipase C pathway seems to play a significant role in HIV-1 Tat-mediated cell death (Haughey et al., 1999). Inhibition of intracellular Ca^{2+} release confers protection against HIV-1 Tat-

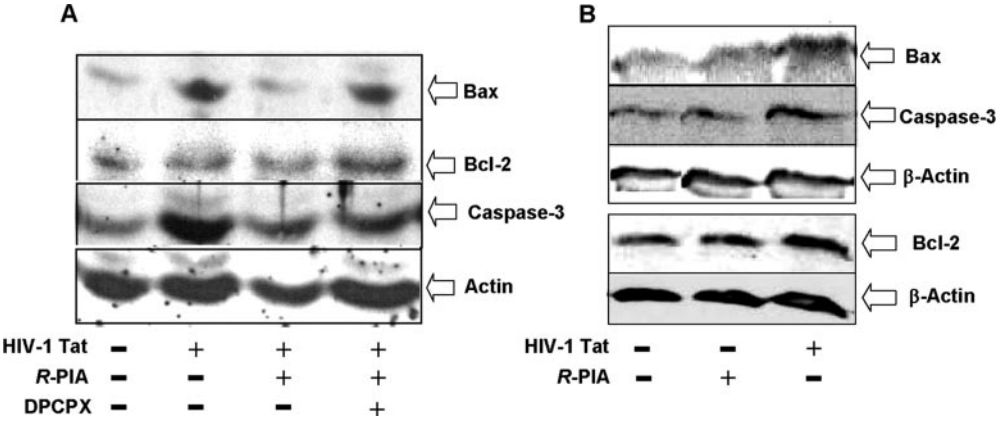

Fig. 7. Activation of the A_1AR reduces the increases in Bax and caspase-3 in response to HIV-1 Tat. A, PC12 cells were treated with HIV-1 Tat (100 nM), R-PIA (1 μM), and DPCPX (1 μM) for 18 h. Cells were lysed, and lysates were subjected to Western blotting using polyclonal antibodies against Bcl-2, Bax, and caspase-3. B, lack of effect of R-PIA on basal levels of Bax, Bcl-2, and caspase-2. β-Actin was used as a loading control for normalization. All the experiments were repeated at least three times.

induced death in primary neuron cultures (Haughey et al., 1999). Tat mediates a biphasic increase in intracellular Ca^{2+} in primary neuron cultures. There seems to be a rapid increase, presumably the activation of phospholipase C and inositol phosphate-3 release, and a later response mediated through a plasma membrane glutamate receptor (Haughey et al., 1999). This latter response was inhibited by glutamate receptor antagonist and was dependent on the initial rapid increase in intracellular Ca^{2+} (Haughey et al., 1999). A recent study also implicates Ca^{2+} uptake into mitochondria in Tat-dependent toxicity (Langford et al., 2004).

Because this response was inhibited by pertussis toxin, an inhibitor of the guanine nucleotide regulatory protein G_i, the investigators (Haughey et al., 1999) concluded that the increase in intracellular Ca^{2+} indicates that Tat interacts with a plasma membrane site coupled to G_i and activation of phospholipase C. However, recent evidence indicates that inhibition of Tat intra- and extracellular functions, such as activation of NF-κB, HIV-1 long terminal repeat transactivation, and transforming growth factor-β production, are inhibited by the B-oligomer of pertussis toxin, which is devoid of ADP ribosyltransferase activity (Rizzi et al., 2004; Zocchi et al., 2005). This suggests that the conclusion of an association of the Tat plasma membrane "receptor" with G_i may be incorrect. In addition, these data would suggest that the effect of B-oligomer would be additive to or would potentiate the inhibition of Tat signaling by the A_1AR.

The mechanism by which activation of the A_1AR inhibits intracellular Ca^{2+} release in neuronal cell types is currently being explored. In cardiac tissue, however, activation of the A_1AR decreases sarcoplasmic Ca^{2+} uptake and serves to reduce Ca^{2+} overload during ischemia (Zucchi et al., 2002). This receptor also mediates the activation of mitochondrial K_{ATP} channels, a mechanism that could underlies its importance in ischemic preconditioning (Yoshida et al., 2004). Activation of mitochondrial K_{ATP} presumably decreases the driving force for Ca^{2+} entry into the mitochondria via a Ca^{2+} uniporter (Liu et al., 1998). It is interesting that the toxic effect of Tat is attenuated by blocking mitochondrial Ca^{2+} uptake (Langford et al., 2004), even though in these studies, blockade of endoplasmic reticulum Ca^{2+} flux was not effective.

Two targets of Tat-induced intracellular Ca^{2+} release are the constitutive forms of NOS, such as endothelial and neuronal NOS. The activity of both of these NOS isoforms is stimulated by an increase in intracellular Ca^{2+} (Moncada et al., 1991). The resulting NO produced could mediate some of the cytotoxicity of HIV-1 Tat. Ca^{2+} could also mediate the activation of NF-κB, leading to a more delayed induction of iNOS. The iNOS gene is predominantly regulated at the level of transcription via several putative NF-κB response elements (Chen et al., 2005) and AP-1 regulatory sites (Cho et al., 2005). Although HIV-1 Tat is known to activate NF-κB (Conant et al., 1996), our data implicate a Tat-mediated increase in intracellular Ca^{2+} as an important mediator of this process. Activation of NF-κB by bacterial lipopolysaccharide and pertussis toxin B-oligomer in mouse macrophages (RAW 264.7) and hamster ductus deferens (DDT_1 MF-2) cell line, respectively, is also dependent on an increase in intracellular Ca^{2+} (Jajoo et al., 2006; Martin et al., 2006). Thus, inhibition of intracellular Ca^{2+} release could serve as the primary target of adenosine, which is manifested in decreased activation of NF-κB, reduced iNOS expression, and NO release. We observed that HIV-1 Tat also increased AP-1 DNA binding activity but that this response was not inhibited (but was enhanced) by A_1AR activation. This suggests specificity for A_1AR downstream signaling to modulate NF-κB but not AP-1 activity, at least in the PC12 cells.

NO promotes neurotoxicity (Jaffrey and Snyder, 1995) and plays an important role in mediating HIV-D (Adamson et al., 1996). The neurotoxicity derives in part from the reaction of NO with superoxide anions to form peroxynitrite and to

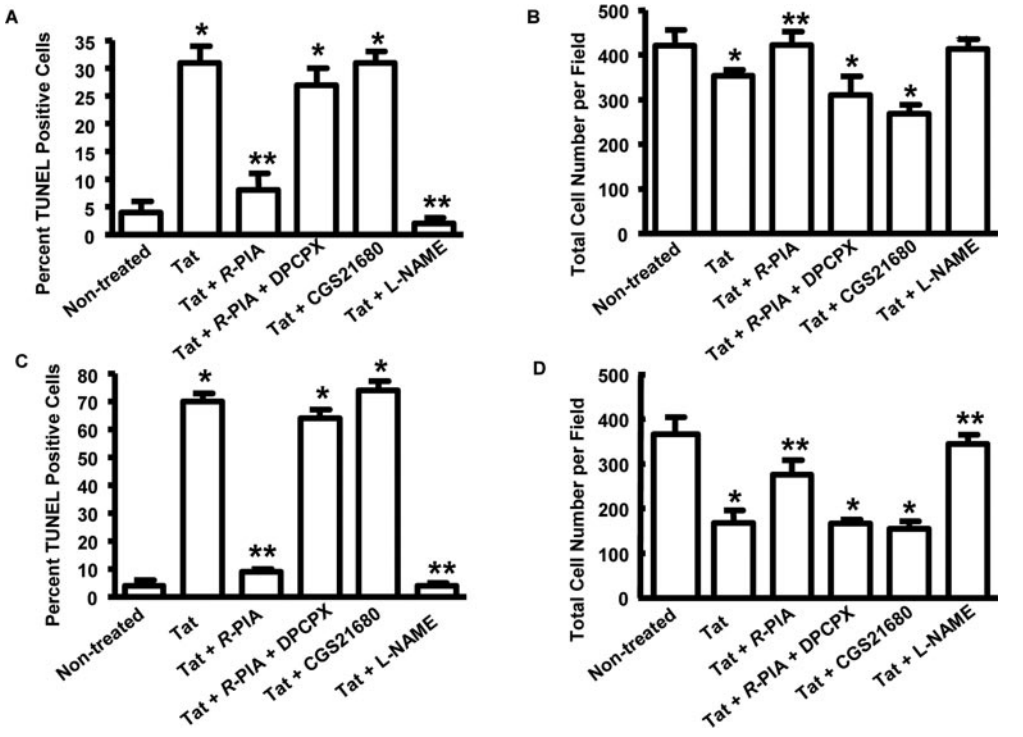

Fig. 8. Inhibition of HIV-1 Tat-mediated apoptosis in CGNs by activation of the A_1AR. Apoptotic cells were visualized by TUNEL assays, according to the manufacturer's instructions (Intergen, Purchase, NY). The percentage of TUNEL-positive cells (brown) were assessed by the analysis of digitized images from 12 or more microscopic fields of TUNEL-stained cells. A and C, percentage of TUNEL-positive cells is presented after 24- and 72-h Tat treatment, respectively. B and D, the total number of cells per field after Tat and/or the indicated drugs (1 μM concentration each for the adenosine analogs and 250 mM L-NAME) treatment for 24 and 72 h, respectively. *, statistically significant difference from control. **, statistically significant difference from Tat-treated groups ($p < 0.05$), respectively. The effects of Tat + R-PIA + DPCPX in B, C, and D were statistically different from those obtained with Tat + R-PIA + Tat alone ($p < 0.05$).

increased nitrosylation of cellular proteins to alter their functions (Kruman et al., 1998). Our data provide ample evidence that NO contributes to neuronal apoptosis, because inhibition of NOS by L-NAME reduces Tat-mediated apoptosis. In addition, we demonstrate that neurons could be directly injured by the NO they produce in response to HIV-Tat and do not necessarily have to depend on NO released by activated immune cells.

Tat has been shown to mediate apoptosis in PC12 cells at doses similar to the ones used in our study (Gavriil et al., 2000; Wong et al., 2005). Higher concentrations of Tat were used in one study to induce apoptosis in CGNs (Ramirez et al., 2001). However, these investigators stated that the effective dose is much lower because a significant fraction of Tat is lost during preparation and administration of the agent. HIV-1 shows little viral gene expression in the cerebellum, but this brain region has the long terminal repeat CCAAT/enhancer-binding protein site II 4C that promotes the accumulation of latent provirus (Burdo et al., 2004). Despite this, HIV-1 infection of the cerebellum has been associated with ataxia and myoclonus (Canafoglia et al., 2003) attributable to cerebellar dysfunction. Furthermore, neuropathological findings demonstrate that α-amino-3-hydroxy-5-methyl-4-isoxazolepropionic acid receptor expression is dramatically reduced in cerebellar tissue from patients with HIV-D (Everall et al., 1995), and preclinical studies demonstrate that cerebellar granule cells are the target of HIV-1 virotoxins such as gp120 (Bachis and Mocchetti, 2004).

Although the exact mechanism of Tat-induced apoptosis is not clear, various pieces of evidence have implicated increased expression of Fas ligand, an apoptosis effector molecule, activation of cyclin-dependent kinases, up-regulation of caspases (Kruman et al., 1998), increased levels of the proapoptotic protein Bim, and decreased levels of antiapoptotic protein Bcl-2 as potential mediators (Kaul et al., 2001). As such, we extended our investigation to determine the effect of A_1AR activation on the levels of the proapoptotic protein Bax and the antiapoptotic protein Bcl-2. An imbalance in expression between these two proteins in mitochondrial membranes leads to cytochrome *c*-mediated apoptosis (Reed, 1997). Because the expression of Bax in primary cultures of cortical neurons is dependent on NF-κB activation (Shou et al., 2002), we speculated that HIV-1 Tat would increase its expression, and that A_1AR activation would inhibit this response. We observed no effect of HIV-Tat on Bcl-2 protein expression but increased expression of proapoptotic Bax. This increased Bax/Bcl-2 ratio probably triggers apoptosis in these cells. Activation of the A_1AR attenuated Tat-mediated increase in Bax expression, which should normalize the Bax/Bcl-2 ratio and thereby attenuate apoptosis.

A consequence of Bax/Bcl-2 imbalance is the initiation of the apoptotic cascade by HIV-Tat and activation of caspases (Bartz and Emerman, 1999). We show that caspase-3, an important molecule in the neuronal apoptotic cascade (Kruman et al., 1998), is induced by HIV-1 Tat and that A_1AR activation attenuated this response. It is interesting that NO donors (sodium nitroprusside and SNAP) also activate caspase-3 and induce apoptosis in chromaffin cells (Vicente et al., 2006) and promote apoptosis in primary cultures of cortical neurons (as shown in this study), consistent with the hypothesis that NO mediates the apoptotic response to HIV-Tat in PC12 and neuronal cultures.

An interesting observation made in this study is that HIV-Tat induces A_1AR expression. This observation seems contradictory because Tat mediates apoptosis of these cells, which is countered by A_1AR activation. However, induction of the A_1AR could represent a compensatory response to maintain cell viability. We have observed a similar response to stress in different cell lines, which was mediated by NF-κB (Pingle et al., 2004; Jajoo et al., 2006). Likewise, activation of NF-κB by HIV-1 Tat seems essential for the induction of the A_1AR in PC12 cells. An important question raised by our findings is determining the exact role of NF-κB activation by HIV-Tat in these cells. On the one hand, it promotes iNOS (and NO production) and Bax expression, which contribute to cytotoxicity. On the other hand, NF-κB activation also increases A_1AR expression, which mediates a cytoprotective effect. The fate of neurons is probably decided by a balance between the prosurvival and neurotoxic molecules regulated directly by this transcription factor. Therefore, the activation of the A_1AR by exogenous agonist pushes the cells away from apoptosis and toward a path for survival.

It is already known that levels of adenosine, and ultimately the activation of the A_1AR in the central nervous system, increase significantly after metabolic insults (Rubio et al., 1975). Although these increases confer some degree of neuroprotection, exogenously applied adenosine analogs could provide additional protection in conditions such as HIV-induced toxicity. It is generally believed that activation of the A_1 and A_3AR protects cells from toxic insults, whereas activation of the A_{2A}AR in the brain seems to aggravate injury (Ramkumar et al., 2001). Hence, exogenously applied drugs to decrease HIV-1 neurotoxicity should target the A_1AR, the predominant AR subtype in the brain. However, administration of centrally acting A_1AR agonists is associated with a significant degree of sedation (Dunwiddie and Masino, 2001), an undesirable side effect in an outpatient setting. Other strategies for increasing extracellular brain concentrations of adenosine include inhibition of its transport or inhibition of its incorporation back into ATP using adenosine kinase inhibitors (Boison, 2005).

In summary, data from our study demonstrate that the A_1AR could serve as a novel target to counter HIV neurotoxicity by inhibiting an NF-κB-dependent induction of iNOS and thereby reduce NO cytotoxicity. Exogenous application of receptor-selective agonist and/or preserving endogenous adenosine could augment cytoprotective mechanisms mediated by adenosine and the A_1AR.

Acknowledgments

We thank Dr. Greg Brewer for providing cultures of rat embryonic cortical neurons. HIV-1 Tat was obtained through the National Institutes of Health AIDS Research and Reference Reagent Program.

References

Adamson DC, Wildemann B, Sasaki M, Glass JD, McArthur JC, Christov VI, Dawson TM, and Dawson VL (1996) Immunologic NO synthase: elevation in severe AIDS dementia and induction by HIV-1 gp41. *Science* **274:**1917–1921.

Bachis A and Mocchetti I (2004) The chemokine receptor CXCR4 and not the N-methyl-D aspartate receptor mediates gp120 neurotoxicity in cerebellar granule cells. *J Neurosci Res* **75:**75–82.

Bartz SR and Emerman M (1999) Human immunodeficiency virus type 1 Tat induces apoptosis and increases sensitivity to apoptotic signals by up-regulating FLICE/caspase-8. *J Virol* **73:**1956–1963.

Boison D (2005) Adenosine and epilepsy: from therapeutic rationale to new therapeutic strategies. *Neuroscientist* **11:**25–36.

Bradford MM (1976) A rapid and sensitive method for the quantitation of microgram

quantities of protein utilizing the principle of protein-dye binding. *Anal Biochem* **72:**248–254.
Brewer GJ, Torricelli JR, Evege EK, and Price PJ (1993) Optimized survival of hippocampal neurons in B27-supplemented Neurobasal, a new serum-free medium combination. *J Neurosci Res* **35:**567–576.
Burdo TH, Gartner S, Mauger D, and Wigdahl B (2004) Region-specific distribution of human immunodeficiency virus type 1 long terminal repeats containing specific configurations of CCAAT/enhancer-binding protein site II in brains derived from demented and nondemented patients. *J Neurovirol* **10:**7–14.
Canafoglia L, Panzica F, Franceschetti S, Carriero MR, Ciano C, Scaioli V, Chiapparini L, Visani E, and Avanzini G (2003) Rhythmic cortical myoclonus in a case of HIV-related encephalopathy. *Mov Disord* **18:**1533–1538.
Chen YJ, Hsu KW, Tsai JN, Hung CH, Kuo TC, and Chen YL (2005) Involvement of protein kinase C in the inhibition of lipopolysaccharide-induced nitric oxide production by thapsigargin in RAW 264.7 macrophages. *Int J Biochem Cell Biol* **37:**2574–2585.
Cho IJ, Lee AK, Lee SJ, Lee MG, and Kim SG (2005) Repression by oxidative stress of iNOS and cytokine gene induction in macrophages results from AP-1 and NF-kappaB inhibition mediated by B cell translocation gene-1 activation. *Free Rad Biol Med* **39:**1523–1536.
Conant K, Ma M, Nath A, and Major EO (1996) Extracellular human immunodeficiency virus type 1 Tat protein is associated with an increase in both NF-kappa B binding and protein kinase C activity in primary human astrocytes. *J Virol* **70:**1384–1389.
Dunwiddie TV and Masino SA (2001) The role and regulation of adenosine in the central nervous system. *Annu Rev Neurosci* **24:**31–55.
Everall IP, Hudson L, al-Sarraj S, Honavar M, Lantos P, and Kerwin R (1995) Decreased expression of AMPA receptor messenger RNA and protein in AIDS: a model for HIV associated neurotoxicity. *Nat Med* **1:**1174–1178.
Faure M, Voyno-Yasenetskaya TA, and Bourne HR (1994) cAMP and $\beta\gamma$ subunits of heterotrimeric G proteins stimulate the mitogen-activated protein kinase pathway in COS-7 cells. *J Biol Chem* **269:**7851–7854.
Fotheringham J, Mayne M, Holden C, Nath A, and Geiger JD (2004) Adenosine receptors control HIV-1 Tat-induced inflammatory responses through protein phosphatase. *Virology* **327:**186–195.
Gavriil ES, Cooney R, and Weeks BS (2000) Tat mediates apoptosis in vivo in the rat central nervous system. *Biochem Biophys Res Commun* **267:**252–256.
González-Scarano F, and Martin-Garcia J (2005) The neuropathogenesis of AIDS. *Nat Rev Immunol* **5:**69–81.
Guroff G, Dickens G, End D, and Londos C (1981) The action of adenosine analogs on PC12 cells. *J Neurochem* **37:**1431–1439.
Haughey NJ, Holden CP, Nath A, and Geiger JD (1999) Involvement of inositol 1,4,5 trisphosphate-regulated stores of intracellular calcium in calcium dysregulation and neuron cell death caused by HIV-1 protein tat. *J Neurochem* **73:**1363–1374.
Jaffrey SR and Snyder SH (1995) Nitric oxide: a neural messenger. *Annu Rev Cell Dev Biol* **11:**417–440.
Jajoo S, Mukherjea D, Pingle S, Sekino Y, and Ramkumar V (2006) Induction of adenosine A1 receptor expression by pertussis toxin via an adenosine 5′-diphosphate ribosylation independent pathway. *J Pharmacol Exp Ther* **317:**1–10.
Jones M, Olafson K, Del Bigio MR, Peeling J, and Nath A (1998) Intraventricular injection of human immunodeficiency virus type 1 (HIV-1) tat protein causes inflammation, gliosis, apoptosis, and ventricular enlargement. *J Neuropathol Exp Neurol* **57:**563–570.
Kaul M, Garden GA, and Lipton SA (2001) Pathways to neuronal injury and apoptosis in HIV-associated dementia. *Nature* **410:**988–994.
Kruman II, Nath A, and Mattson MP (1998) HIV-1 protein Tat induces apoptosis of hippocampal neurons by a mechanism involving caspase activation, calcium overload, and oxidative stress. *Exp Neurol* **154:**276–288.
Kumar A, Manna SK, Dhawan S, and Aggarwal BB (1998) HIV-Tat protein activates c-Jun N-terminal kinase and activator protein-1. *J Immunol* **161:**776–781.
Langford D, Grigorian A, Hurford R, Adame A, Crews L, and Masliah E (2004) The role of mitochondrial alterations in the combined toxic effects of human immunodeficiency virus Tat protein and methamphetamine on calbindin positive-neurons. *J Neurovirol* **10:**327–337.
Liu Y, Sato T, O'Rourke B, and Marban E (1998) Mitochondrial ATP-dependent potassium channels: novel effectors of cardioprotection? *Circulation* **97:**2463–2469.
Martin L, Pingle SC, Hallam DM, Rybak LP, and Ramkumar V (2006) Activation of the adenosine A_3 receptor in RAW 264.7 cells inhibits lipopolysaccharide-stimulated tumor necrosis factor-alpha release by reducing calcium-dependent activation of nuclear factor κB and extracellular signal-regulated kinase 1/2. *J Pharmacol Exp Ther* **316:**71–78.
Moncada S, Palmer RM, and Higgs EA (1991) Nitric oxide: physiology, pathophysiology, and pharmacology. *Pharmacol Rev* **43:**109–142.
Nath A, Haughey NJ, Jones M, Anderson C, Bell JE, and Geiger JD (2000) Synergistic neurotoxicity by human immunodeficiency virus proteins Tat and gp120: protection by memantine. *Ann Neurol* **47:**186–194.
Nie Z, Mei Y, Malek RL, Marcuzzi A, Lee NH, and Ramkumar V (1999) A role of p75 in NGF-mediated down-regulation of the A_{2A} adenosine receptors in PC12 cells. *Mol Pharmacol* **56:**947–954.
New DR, Maggirwar SB, Epstein LG, Dewhurst S, and Gelbard HA (1998) HIV-1 Tat induces neuronal death via tumor necrosis factor-α and activation of non-N-methyl D-aspartate receptors by a NFκB-independent mechanism. *J Biol Chem* **273:**17852–17858.
Ochiishi T, Chen L, Yukawa A, Saitoh Y, Sekino Y, Arai T, Nakata H, and Miyamoto H (1999) Cellular localization of adenosine A1 receptors in rat forebrain: immunohistochemical analysis using adenosine A1 receptor-specific monoclonal antibody. *J Comp Neurol* **411:**301–316.
Pingle SC, Mishra S, Marcuzzi A, Bhat SG, Sekino Y, Rybak LP, and Ramkumar V (2004) Osmotic diuretics induce adenosine A1 receptor expression and protect renal proximal tubular epithelial cells against cisplatin-mediated apoptosis. *J Biol Chem* **279:**43157 43167.
Pingle SC, Sanchez JF, Hallam DM, Williamson AL, Maggirwar SB, and Ramkumar V (2003) Hypertonicity inhibits lipopolysaccharide-induced nitric oxide synthase expression in smooth muscle cells by inhibiting nuclear factor κB. *Mol Pharmacol* **63:**1238–1247.
Ramirez SH, Sanchez JF, Dimitri CA, Gelbard HA, Dewhurst S, and Maggirwar SB (2001) Neurotrophins prevent HIV Tat-induced neuronal apoptosis via a nuclear factor-kappa B (NF-κB)-dependent mechanism. *J Neurochem* **78:**874–889.
Ramkumar V, Hallam DM, and Nie Z (2001) Adenosine, oxidative stress and cytoprotection. *Jpn J Pharmacol* **86:**265–274.
Reed JC (1997) Double identity for proteins of the Bcl-2 family. *Nature* **387:**773–776.
Ren H and Stiles GL (1995) Separate promoters in the human A1 adenosine receptor gene direct the synthesis of distinct messenger RNAs that regulate receptor abundance. *Mol Pharmacol* **48:**975–980.
Rizzi C, Alfano M, Bugatti A, Camozzi M, Poli G, and Rusnati M (2004) Inhibition of intra- and extra-cellular Tat function and HIV expression by pertussis toxin B-oligomer. *Eur J Immunol* **34:**530–536.
Robinson AJ and Dickenson JM (2001) Regulation of the p42/p44 MAPK and p38 MAPK by the adenosine A_1 receptor in DDT_1MF-2 cells. *Eur J Pharmacol* **413:**151–161.
Rubio R, Berne RM, Bockman EL, and Curnish RR (1975) Relationship between adenosine concentration and oxygen supply in rat brain. *Am J Physiol* **228:**1896–1902.
Schwarze SR, Ho A, Vocero-Akbani A, and Dowdy SF (1999) In vivo protein transduction: delivery of a biologically active protein into the mouse. *Science* **285:**1569–1572.
Shou Y, Li N, Li L, Borowitz JL, and Isom GE (2002) NF-kappaB-mediated upregulation of Bcl-X(S) and Bax contributes to cytochrome c release in cyanide-induced apoptosis. *J Neurochem* **81:**842–852.
Sui Z, Kovacs AD, and Maggirwar SB (2006) Recruitment of active glycogen synthase kinase-3 into neuronal lipid rafts. *Biochem Biophys Res Commun* **345:**1643–1648.
Vicente S, Perez-Rodriguez R, Olivan AM, Martinez Palacian A, Gonzalez MP, and Oset Gasque MJ (2006) Nitric oxide and peroxynitrite induce cellular death in bovine chromaffin cells: evidence for a mixed necrotic and apoptotic mechanism with caspases activation. *J Neurosci Res* **84:**78–96.
Wong K, Sharma A, Awasthi S, Matlock EF, Rogers L, Van Lint C, Skiest DJ, Burns DK, and Harrod R (2005) HIV-1 Tat interactions with p300 and PCAF transcriptional coactivators inhibit histone acetylation and neurotrophin signaling through CREB. *J Biol Chem* **280:**9390–9399.
Yoshida M, Nakakimura K, Cui YJ, Matsumoto M, and Sakabe T (2004) Adenosine A_1 receptor antagonist and mitochondrial ATP sensitive potassium channel blocker attenuate the tolerance to focal cerebral ischemia in rats. *J Cereb Blood Flow Metab* **24:**771–779.
Zocchi MR, Contini P, Alfano M, and Poggi A (2005) Pertussis toxin (PTX) B subunit and the nontoxic PTX mutant PT9K/129G inhibit tat-induced TGF-β production by NK cells and TGF-β-mediated NK cell apoptosis. *J Immunol* **174:**6054–6061.
Zucchi R, Gerniway RJ, Ronca-Testoni S, Morrison RR, Ronca G, and Matherne GP (2002) Effect of cardiac A1 adenosine receptor overexpression on sarcoplasmic reticulum function. *Cardiovasc Res* **53:**326–333.

Address correspondence to: Dr. Vickram Ramkumar, Department of Pharmacology, Southern Illinois University School of Medicine, PO Box 19629, Springfield, IL 62794-9629. E-mail: vramkumar@siumed.edu